Classical equations-of-motion model for high-energy heavy-ion collisions

G. S. Anagnostatos
Department of Physics and Astronomy, University of Maryland, College Park, Maryland 20742 and Institute of Nuclear Physics, "DEMOKRITOS" National Research Center for Physical Sciences, Aghia Paraskevi 15310, Greece
(Received 7 July 1987)

A classical nonrelativistic microscopic model for high-energy heavy-ion collisions is presented, based on equations-of-motion calculations, where all the nucleon trajectories are computed with suitable two-body forces between all pairs of nucleons in the target and projectile. Comparison with experiment and with the results of other models is made. The model considers both position and velocity configurations according to a nuclear structure model, the isomorphic shell model previously and independently published. Thus, its results are objective and completely reproducible. The main feature, however, relies on the properties of the two-body potential used in the model which reproduces both the transverse momentum transfer cross section and the longitudinal momentum loss cross section, and at the same time possesses good saturation properties. While the present model uses a nonrelativistic approach, its results are comparable to those of other models using relativistic approaches.

I. INTRODUCTION

High-energy (HE) heavy-ion (HI) collisions is a subject of growing interest in nuclear physics. This comes from the indications that pion condensation, density isomers, quark-gluon plasma, nuclear shock waves, and other exotic phenomena may appear in the course of these reactions. A complete relativistic quantum-mechanical handling of such reactions should be the most desirable approach. Since such an approach, unfortunately, is not possible, one resorts to classical or semiclassical approaches.

On the basis of specific initial conditions and appropriate choice of NN interaction it has been shown[1-3] that the equations of classical mechanics could be used to determine the motion of each nucleon of the target-projectile system. The easiest models for calculations are the fireball[2] and firestreak[3] models assuming the simplest collision geometry and thermal equilibrium. Hydrodynamical models[4] are more realistic, taking into account the compressibility, viscosity, heat conductivity of nuclear matter, and local thermal equilibrium. They are based on local relativistic energy-momentum conservation and on the equation of state of the nuclear matter. Among them the two-fluid models are more realistic. The simplest microscopic models are the cascade models[5-7] and the models using the Boltzmann equation.[8] The most microscopic models are those based on the classical equation of motion approach which can be relativistic[9] or nonrelativistic,[1,10] depending on the relative velocity between target and projectile. The models offer a dynamically consistent description of the surface effects and the fragmentation process. The classical equation of motion approach is essentially the molecular dynamics approach which assumes a classical description valid for bombarding energies > 100 MeV/nucleon.

The introduction of the classical equation of motion approach[1] for the study of HE, HI collisions is due to Bodmer and Panos in 1977. Since then researchers from other groups[11-14] have successfully applied variations of the approach to several reactions. All these variations, however, have more or less the same limitations and defects. The purpose of the present paper is to simultaneously improve all these versions and thus to increase their effectiveness and applicability. For one to comprehend and appreciate these improvements a brief account of the development of the classical equation of motion approach is undertaken below. Because of these improvements and the systematization and simplification of the method reached afterwards, from here on we will refer to the approach as the classical equations-of-motion model, abbreviated as CEMMO. Meson production is not included and the nucleons are taken to be spinless.

II. CLASSICAL EQUATIONS-OF-MOTION MODEL

Implementation of the CEMMO (classical "nonrelativistic" equations-of-motion calculations, where all the nucleon trajectories are computed with suitable two-body forces between all pairs of nucleons) involves seven elements.[1,10]

A. Choice of a two-body potential

The choice of the best possible nucleon-nucleon potential acting between all pairs of nucleons presumably leads (in the model dynamics corresponding to this potential) to the mechanism of the reaction compression and other interesting characteristics. The choice of the potential is made by examining its high- and low-energy properties.

Here, however, there is no simulation of the Pauli principle beyond the consequences coming from the short-range repulsive nature of the potential used. Also, despite the fact that it was possible, the Coulomb interaction is not taken into account, because of its insignificant overall contribution to the results of interest for light nuclei.

Our static central potential consists of a repulsive (R) and an attractive (A) Yukawa-type component, and thus short-range correlations are taken into account automatically. Thus the potential has the form

$$V(r_{ij})=V_R e^{-\mu_R r_{ij}}/r_{ij}-V_A e^{-\mu_A r_{ij}}/r_{ij} , \quad (1)$$

where V_R, V_A, μ_R, and μ_A are the strengths and ranges of the potential components and r_{ij} is the relative distance of nucleons i and j. The values of the constants, from Ref. 15, are

$$V_R=1.7\times10^{17} \text{ MeV/fm}, \quad V_A=187.0 \text{ MeV/fm}$$

and

$$\mu_R=31.8538 \text{ fm}^{-1}, \quad \mu_A=1.3538 \text{ fm}^{-1} .$$

These constants correspond[15] to an effective hard-core radius $r_c=1.13$ fm where $V(r_c)=0$ and to a radius $r_m\cong1.22$ fm at the potential minimum $V(r_m)=-27.5$ MeV.

The high- and low-energy properties of our potential have been successfully tested in Ref. 15. The main difference of this potential from all other potentials used in HE, HI collisions is that it is the best potential which simultaneously reproduces the first *two* moments [$\sigma^{(1)}(E)$, longitudinal momentum loss cross section, and $\sigma^{(2)}(E)$, transverse momentum transfer cross section] of the c.m. differential scattering cross section for free nucleons at high energies, >50 MeV/nucleon, and at the same time possesses very good saturation properties. All other potentials[1,10–14] have been tested with respect to the second moment $\sigma^{(2)}(E)$ only, and possess moderate to poor saturation properties. Thus, it is expected that our potential will be more reliable in describing HE, HI collisions, where both longitudinal and transverse momentum transfers are important. In Ref. 16 a test is made for all similar potentials[10–14,17] published until 1984. In that theoretical test we have firstly estimated the $\sigma^{(1)}(E)$ values for all potentials examined which by construction give acceptable values for $\sigma^{(2)}(E)$, and secondly we have estimated the abilities of these potentials to give reasonable binding energies. For the potentials in the literature subsequent to Ref. 16, a similar test will appear elsewhere, with the same conclusion that the potential of Eq. (1) is superior to all other potentials published so far, regarding their high- and low-energy properties.

However, it is interesting to make some remarks concerning two of the newer potentials.[13,14,18] Kiselev,[13] examining nucleon correlation functions for two of his (P_1,P_2) potentials, gives preference to potential P_2, which has a radius $r_m=1.2$ fm at the potential minimum ($V_m=-30$ MeV). These values are almost identical to our values $r_m\cong1.22$ fm and $V_m=-27.5$ MeV. However, Kiselev even with this potential was unable to obtain simultaneously satisfactory NN scattering and nuclear densities, which is not a problem for our potential.[15,16] Finally, I would like to qualitatively compare the potential of Eq. (1) with the central effective nucleon-nucleon potentials in the $^3S_1$ and $^1S_0$ channels arising from residual color forces.[18] These two potentials, comprising the latest efforts to derive the NN potential from the quark model with chromodynamics,[18] are very similar to each other and to our potential of Eq. (1), since all three potentials have the form of two Yukawa-type components, a core radius r_c between 1.0 and 1.1 fm, and a depth between 22 and 28 MeV. In comparing the potential of Eq. (1) with NN potentials derived from quark cluster models, however, one should remember that for these potentials the addition of a meson theoretical potential is needed in order to fit the NN data.

B. Choice of initial configurations of nucleon positions

The configurations of positions $\bar{r}_1$ are extended from $i=1$ to A_P for the projectile and from $i=A_P+1$ to A_P+A_T for the target, where A_P and A_T are the mass numbers for the target and projectile, respectively. In the literature the majority of researchers[1,10,13,14] choose a random-number-generated configuration of positions (for the target and the projectile) within a sphere equal to the nuclear size, while the remaining researchers[11] consider configurations corresponding to crystalline structures. The former configurations lead to very hot nuclei which contract and evaporate rather fast in comparison to the reaction time,[12] while the latter configurations also have the disadvantage of contraction, since the nucleons drift toward the configuration of minimum energy of the chosen nucleon-nucleon potential. These arguments have been checked by isolating both the target and the projectile and leaving them to evolve according to the NN interaction. Thus, both types of configurations of positions in the literature exhibit undesirable features.

In the present paper, the initial configurations of positions, instead of being created *ad hoc*, are taken according to an existing nuclear structure model, the isomorphic shell model.[19] These configurations have normal densities, include short-range nucleon correlations, and for the potential of the previous section possess correct saturation properties.[15,19] That is, they fulfill all necessary requirements for such initial configurations. These configurations, for the nucleus examined in the present paper and for any nucleus in the *sd* shell, have already been published in Refs. 15 and 16, while for any other nucleus the configurations can be derived from the information given in Fig. 1 of Ref. 19.

The main advantage of the present configurations is that, in addition to fulfilling the above requirements, they come from an independent nuclear structure model[19] and thus they are objective (not *ad hoc*) and available to anyone interested in verifying our results or performing his or her own calculations on HE, HI collisions.

C. Choice of initial configurations of nucleon velocities (momenta)

The configurations of momenta $\bar{p}$ are extended, as are the configurations of positions $\bar{r}$, from $i=1$ to A_P for the projectile and from $i=A_P+1$ to A_P+A_T for the target.

In Refs. 1, 10, 13, and 14 the nucleon velocities are taken at random in direction and magnitude (the corresponding kinetic energies however, are in the range of those for an ideal degenerate Fermi gas), while in Ref. 12 the magnitude of the initial velocities $\bar{u}_i(0)$ is taken from

the relationship $\frac{1}{2}Mu_i^2(0)=E_B-U(r_i)$ [where E_B is the binding energy, M is the nucleon mass, and $U(r)$ is the average potential of a nucleon in a nucleus] and the direction of $\bar{u}_i(0)$ is taken at random, and in Ref. 11 these velocities are taken to be equal to zero. Thus, in all cases in the literature, the velocities are taken more or less randomly. To the contrary, the velocities in the present work[20] come from the same nuclear structure model[19] as the "positions," their magnitudes and directions are consistent with the independent-particle model,[21] and include the uncertainty due to the confinement of nucleons in the nuclear volume.[22]

Specifically, the kinetic energy in the present paper, as in Svenne's paper,[22] is calculated as the sum of the kinetic energy due to confinement of the nucleons in the nuclear volume and of the kinetic energy due to rotation of nucleons. (Here, the rotation of a nucleon refers to the rotation of the average position of this nucleon around its orbital angular momentum axis. Such positions and axes for nuclei up to the end of the *sd* shell are given in detail in Fig. 1 of Ref. 20.) Thus, according to Ref. 22, we have for the kinetic energy of a nucleon

$$\langle T\rangle \geq \hbar^2/2M(1/R_{\max}^2+\langle L^2/\rho^2\rangle)\ , \tag{2}$$

where $R_{\max}$ is the confinement radius of the nucleons, i.e., the radius of the outer-shell nucleon centers (R) plus the radius of the nucleon[20] bag (r_N). M is the nucleon mass, and ρ is the radius of the classical orbit of the average position of a specific nucleon. To be even more specific, we take, as an example, the case of a proton in the $1p$ shell, where (from Ref. 20) $R=2.541$ fm, $r_P=0.860$ fm, and $\rho=2.075$ fm. For this proton from Eq. (2) we obtain $\langle T\rangle \geq 11.4$ MeV. For simplicity, only the equality is considered in any calculation involving this velocity.

Accordingly, the velocity and momentum of any nucleon have two components (uncertainty and orbital components) coming from Eq. (2),

$$\tfrac{1}{2}MV_{\rm unc}^2=\hbar^2/2M(1/R_{\max}^2) \tag{3}$$

and

$$\tfrac{1}{2}MV_{\rm orb}^2=\hbar^2/2M\langle L^2/\rho^2\rangle\ . \tag{4}$$

Now, besides the magnitude of the velocity ($=0.304\times10^{10}$ cm/sec for our example) the complete vector of the orbital component is well specified, since the average position and the orbital angular momentum vector for the particular nucleon are well specified within the isomorphic shell model (see Fig. 1 of Ref. 20). For the uncertainty component, however, the velocity vector could have any (random) direction, but for simplicity we consider the specific direction where $V_x=V_y=V_z=|\bar{V}_{\rm orb}|/\sqrt{3}$ ($=0.105\times10^{10}$ cm/sec for our example).

While in our example the kinetic energy for the specific nucleon comes out to be 11.4 MeV, the nucleon kinetic energies have an average value of about 8 MeV, which means that the average nucleon kinetic energy in the isomorphic shell model is about equal to the average binding energy and thus is substantially different from the Fermi average kinetic energy of about 25 MeV. This large difference with the standard model is more explicitly discussed in the following paragraphs.

The Fermi kinetic energy comes by considering an ideal degenerate Fermi gas, which uniformly fills a sphere of radius $R=r_0A^{1/3}$. In the framework of our approach (classical with an internucleon interaction) this distribution is not the equilibrium one and leads to instability of the nucleus. However, inclusion of the diffuseness of the nuclear boundary leads to a substantial smoothing of the distribution which, together with the *NN* interaction, apparently leads to a shift of mometa toward lower values,[13] that is, towards values closer to ours.

Perhaps the stronger argument in favor of our values is that our kinetic energies (coming from previous, independently published work[20]) have the *unique* advantage of satisfying Koopman's theorem.[23] In addition, from Table II of Ref. 20 (where the kinetic energies for ^{16}O coming from eight papers using different approaches are listed), we see that kinetic energies (from 12.64 to 20.26 MeV) which are higher than our values and approaching the Fermi values lead to very low values (from 2.02 to 6.05 MeV) for the binding energy per particle. Thus, because of the diffuseness of the nuclear boundary and of the *NN* interaction, kinetic energies in the range of Fermi values lead to poor binding energies and do not satisfy Koopman's theorem.

The velocities discussed so far refer to the intrinsic motion of the nucleons and should be redetermined with allowance for the kinetic energy of motion of the approaching nucleus as a whole (external momenta). These initial internal momenta, however, are significant in obtaining a stable nucleus for a time comparable to the reaction time.

D. Choice of an ensemble of initial configurations of positions and momenta

Considering a single initial configuration of positions and momenta for the target and for the projectile, a collision between them is the computer analog of a collision of a single projectile with a single target nucleus. However, our experimental data for such collisions in a specific nuclear reaction is the statistical average of many collisions between projectile and target. Thus, for a realistic computer simulation of the collision, an ensemble of N initial configurations is needed.[10] In the literature the procedure for obtaining an ensemble of configurations from an initial one is either not specified[13] or is taken by arbitrary rotations of the initial configuration.[10] In addition, the number N of configurations in an ensemble is chosen empirically. In the present paper both the procedure for obtaining an ensemble of the initial configuration and the number of configurations in the ensemble are chosen more or less simultaneously and in a precisely specified way.

Considering either random-number distributions[10,13,14] of nucleons in the nuclear volume or considering (as here) nucleon distributions according to the isomorphic shell model,[19] one sees that the distribution of nucleons (par-

ticularly for open-shell nuclei in the isomorphic shell model) in the nuclear volume and specifically on the nuclear surface is not generally uniform. Thus, the procedure for deriving the ensemble from an initial configuration, in combination with the number of distributions in an ensemble, may influence the statistical average of the calculations, if we do not proceed with care.

In the present paper, for the first time, we specify the whole procedure for obtaining the ensemble, in a way independent of the specific nuclear collision. We start by discussing an angular division of both the projectile and the target nuclei. It has been found preferable for this angular division to be the same for the projectile and the target, and independent of the specific nuclei involved. As a first step, we consider any regular polyhedron[24] having a common center with the target nucleus and another (similar) polyhedron having a common center with the projectile. (The relative orientation of the two polyhedra is arbitrary.) As a second step, we assume that the two polyhedra approach each other in *characteristic ways*, e.g., vertices of the one polyhedron approach the vertices, or the center of faces, or the middle of edges of the other, and vice-versa. By deciding which ways of approaching we want, we specify the number (N) of configurations in the ensemble for the specific polyhedron considered. All these N configurations so derived are symmetrically distributed in space. Substituting the polyhedron with another regular polyhedron, the number N is changed, since the numbers of vertices, edges, and faces are different for each polyhedron.[24] To be more quantitative, if our imaginary polyhedron is a tetrahedron (4 vertices), an octahedron (6 vertices), a hexahedron (8 vertices), an icosahedron (12 vertices), a dodecahedron (20 vertices), or an icosidodecahedron (30 vertices), the minimum number N of configurations in our ensemble (considering only the simplest case where vertices of the one polyhedron approach vertices of the other polyhedron) is 4×4, 6×6, 8×8, 12×12, 20×20, or 30×30. Dealing with vertices alone (without considering middles of edges or centers of faces of a polyhedron) is sufficient since, if we want a larger ensemble, it is enough to consider a polyhedron with a larger number of vertices.

We have performed our calculations with a minimum N equal to 16 (for each impact parameter, where the polyhedron has been chosen to be a regular tetrahedron) and the results (see the next section) are satisfying. This is due to the fact that the orientations with which the projectile approaches the target were uniformly distributed in space, and to the fact that the generator configurations of both the target and the projectile satisfy many nuclear properties. Our number $N=16$ should be compared with the numbers $N=25-50$ in Ref. 12, $N=100$ in Ref. 13, and $N=535$ in Ref. 14. Of course, the larger N, the better the statistics. However, any reductions of N save substantial computing time (this is proportional to N), which is a critical factor in calculations of heavy ion collisions. The rather small N which we used in our calculations suffices to provide adequate statistics for single-nucleon inclusive cross sections, but is too small for two or more nucleon correlations[9] by at least an order of magnitude.

E. Many-body dynamical trajectory calculations

These calculations are performed for all $A(=A_P+A_T)$ nucleons of the target-projectile system. For each initial configuration of the ensemble, each impact parameter b, and each laboratory energy E_L, we perform (by using Newton's or Hamilton's equations) dynamical trajectory calculations. These calculations are repeated for each time step and are continued until the collision is effectively over. At each time step we check the total energy of the system, the total linear momentum, and the total angular momentum of the system, which should be conserved during the whole collision. Small deviations (1–2 %) are considered acceptable and it is according to this criterion that the time step is decided.

F. Analysis of trajectories

We first decide on the appropriate binning and the physical quantities of interest, while in the calculations of the cross sections we distinguish between lower and higher energies[25] of products in the following sense. It has been found preferable for the momentum required in the calculation of the cross sections for the lower energies to be evaluated by using $p^2=2mE$, while for the higher energies by using $E^2=p^2c^2+m^2c^4$. This procedure is used here just for the calculation of the final cross section from the nuclear momenta, which are calculated nonrelativistically from the classical trajectory calculations. This use of different momentum expressions dependent on the energy is inspired by a similar treatment in Ref. 9 from which we also take the dividing energy (290 MeV). In Ref. 9 (the results of which we use for comparison), when the relative energy of a nucleon pair is below 290 MeV, nonrelativistic kinematics is used, whereas above this limit the kinematics is taken to be relativistic.

For the final calculations of the proton inclusive cross sections around a specific angle (e.g., around 90°) a numerical integration for each energy over all impact parameters is made. In our calculations, we have considered ten impact parameters from 0.0 to $1.8R$ with a step $0.2R$ (where R is the nuclear radius).

G. Stability of computer simulation for the target and projectile nuclei

Before carrying out calculations of nuclear collisions, we should examine how stable an individually modeled nucleus is, as far as its main properties, e.g., radius, binding energy, conservation of momenta, etc., are concerned. Many potentials in the literature have the defect that a considerable number of nucleons lose kinetic energy rather quickly and come to be spaced in the neighborhood of the minimum point of the two-body potential (contraction), while other nucleons acquire kinetic energy and evaporate. It is of great importance to minimize both the contraction and evaporation for both the target and projectile nuclei, for a time at least longer than the collision time, in order for the results of calculations to be significant. Moreover, for times characteristic of the collision of the two nuclei (e.g., nuclear diameter divided by the velocity of light, i.e., $=15-30$ fm/c), the main nu-

clear properties of each of the noninteracting projectile and target nuclei, besides the total energy of the system, should be conserved, i.e., $\sum \bar{p}_i = 0$, and $\sum_i [\bar{r}_i, \bar{p}_i] = 0$, that is, the linear and angular momenta should be conserved.

Molitoris' nuclei[14] assume crystalline structure and Fermi random momenta, and are stable for typical collision times of about 30 fm/c. However, these nuclei do not conserve momenta.[14] Our isomorphic shell-model nuclei,[19] assuming nucleon and momenta distributions as in Secs. II B and II C, respectively, and governed by the two body-potential in Sec. II A, conserve momentum and have moderate contraction and evaporation properties. For example, in the cases of nuclei from ^{16}O to ^{40}Co the deviation from conservation of momentum does not exceed 1–2%, the evaporation starts after 10–15 fm/c and the contraction at the same time is about 2% of the rms nuclear radius.

The initial separation between target and projectile is of interest. Theoretically it should suffice to initially separate the nuclei so that they are outside each others force range. In fact, specifically for our model where contraction and evaporation are limited for a rather long time, it is sufficient to let target and projectile initially be just outside each others force range independently of the laboratory relative velocity.

III. CALCULATIONS AND DISCUSSION

On the basis of a potential, that of Eq. (1), the model permits discussion of the main dynamical stages of the collision process: the approach of the nuclei, overlapping of the nuclei, propagation of excitation within the system, and breakup of the system into fragments; i.e., discussion of the whole evolution of the collision. In our calculations the process of fragment production (which depends on the potential used[9]) was not taken into account.

As an example we consider the reaction ^{20}Ne+^{20}Ne at a laboratory energy of 800 MeV/nucleon. This energy (moderately relativistic) is intermediate between energies of a few hundreds of MeV and GeV, and in Refs. 9 and 26 is treated relativistically. A relativistic microscopic approach of this reaction is really more realistic, since such treatment anticipates the multiple production of Δ isobars and π mesons which accompany the products of this reaction. These products influence the dynamics of the process to a large degree. Here, such products are not studied and we restrict ourselves to the determination of the inclusive proton cross sections and of the inclusive cross sections as a function of impact parameter, without going into the various aspects of the complex dynamics of relativistic collisions. For example, in describing the approach of the colliding nuclei, their Lorentz-contraction is not considered and no retarded interaction is used. In general, no relativistic corrections have been made. Relativity has also not been used for two-nucleon scattering in deriving[15] our potential [Eq. (1)]. However, only in the calculations of the final cross-sections do we distinguish between lower and higher energies of products by taking the momenta from $p^2 = 2mE$ and $E^2 = p^2c^2 + m^2c^4$, respectively. In all other cases the nuclear momenta are determined nonrelativistically from the classical trajectory calculation. The use of our simplified approach for modeling various features which have essentially quantum relativistic character can be considered only as a first approximation. Comparison with experiments is not sufficient and can only be a crude justification.

The difference in numerical realization between standard treatments, e.g., as in Refs. 9 and 26 (where the calculations require large computation times), and our approach is significant. For example, calculation of a single collision of an α particle with a Pb nucleus in Ref. 9 takes about 30–40 min of BESM-6 computer time; thus, for the 100–200 collisions required, 50–100 h of the BESM-6 computer time is needed. This should be compared with only 15 h in our PRIME 9955 computer for the reaction Ne+Ne.

Our results on the inclusive proton cross sections coming from our simplified approach are compared in Fig. 1 with experimental data[27] and with the results of Refs. 9 and 26, where a relativistic treatment is considered. One may see the relative successes of the three approaches

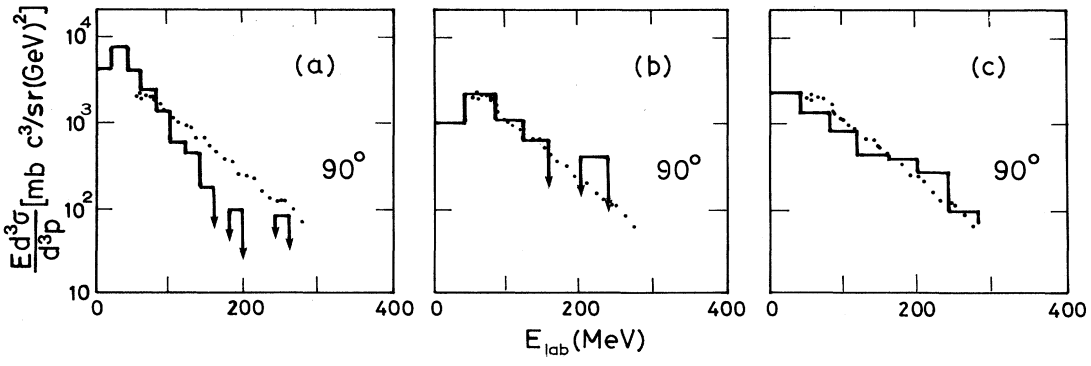

FIG. 1. Invariant inclusive double-differential cross section for the emission of protons in the reaction ^{20}Ne+^{20}Ne at a bombarding energy of $E/A = 800$ MeV/nucleon. Dots represent the experimental results of Nagamiya *et al.* for the system ^{20}Ne+NaF (Ref. 27). (a) shows the histogram coming from the calculation in Ref. 26, while (b) shows that coming from Ref. 9. Finally, (c) shows the histogram coming from our calculations. All cross sections are detected at an angular range of about 90°.

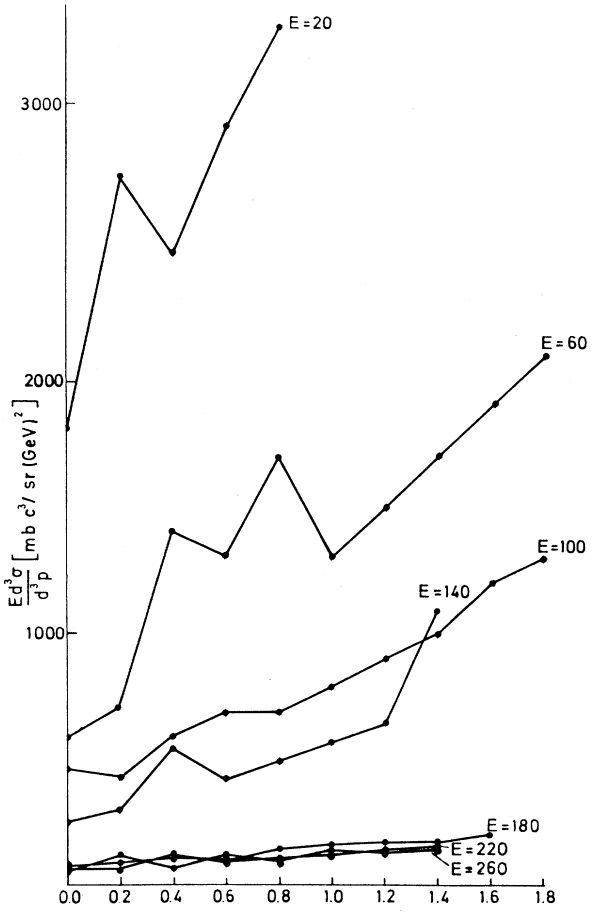

FIG. 2. Inclusive cross section as a function of impact parameter for the emission of protons in the reaction $^{20}Ne+^{20}Ne$ at a bombarding energy of $E/A=800$ MeV/nucleon. Energy (MeV) of inclusive protons is taken as a parameter in the present figure. Inclusive cross section is equal to zero for $E=20$ MeV and $b\geq 1.2$; $E=140$ MeV and $b\geq 1.6$; $E=180$ MeV and $b\geq 1.8$; $E=220$ MeV and $b\geq 1.6$; and $E=260$ MeV and $b\geq 1.6$. The value of inclusive cross section for $E=20$ MeV and $b=1.0$ is 7900 mb c³/sr(GeV)², but it is omitted from the figure for reasons of scale.

presented in Figs. 1(a)–1(c). In making this comparison, however, one should keep in mind the approximations made in each of the three approaches. One notes, however, that our results, just as the results from Ref. 26, do not show the tendency of the experimental data to decrease at very low energies (0–40 MeV), while the results from Ref. 9 agree with these low-energy data. The reason why this decrease does not appear here or in Ref. 26 is discussed in Ref. 9: two-body cluster emission has not been considered at these energies.[9]

Our results on inclusive cross sections as a function of impact parameter are shown in Fig. 2. There are no experimental data for comparison. However, some qualitative remarks can be made. Specifically, we see that the dependence of the inclusive cross sections on impact parameter is much stronger for low energies (up to $E=140$ MeV) than for higher energies.

IV. CONCLUSIONS

The present approach, while nonrelativistic, gives results on inclusive proton cross sections for Ne+Ne collisions at 800 MeV/nucleon which are comparable with those of Refs. 9 and 26, which are relativistic. In this comparison one should consider, of course, the approximations made in each study. It is of interest that the computer realization of the present approach is very much more economical than the existing relativistic approaches,[9,26] at least for the present intermediate energy.

The main characteristic of the present calculations (which closely follow the original work by Bodmer and Panos) is that they are completely reproducible. Anyone could repeat our calculations and could obtain identical results. This is because instead of the random position and momentum distributions (which also lead to large ensembles of initial distributions and, consequently, to large computing times), all our distributions come from a nuclear structure model, the isomorphic shell model,[19] previously and independently published.

While the present approach has been demonstrated here by using a specific reaction, it is valid for any reaction. The configurations of positions and momenta for any nucleus could again be taken from the isomorphic shell model.

ACKNOWLEDGMENTS

The author is greatly indebted to Professor J. J. Griffin of the University of Maryland for the invitation to join the Nuclear Theory Group of his University and for the many valuable and stimulating discussions we had on the subject of this work. My gratitude is extended to all physicists and secretaries of the Nuclear Theory Group for their hospitality and their generous assistance during my rewarding stay there. I am also indebted to Professor C. N. Panos for his very valuable assistance, as an expert on the subject, during the early stages of the present work and for his granting me his computer codes on the CEMMO approach. Finally, I would like to acknowledge that this work could not have taken place without the financial support granted to me by the Fulbright Foundation.

[1]A. R. Bodmer and C. N. Panos, Phys. Rev. C **15**, 1342 (1977).
[2]G. D. Westfall, J. Gosset, P. J. Johansen, A. M. Poskanzer, and W. G. Meyer, Phys. Rev. Lett. **37**, 1202 (1976).
[3]W. D. Myers, Nucl. Phys. **A296**, 177 (1978).
[4]A. A. Amsden, A. S. Goldhaber, F. H. Harlow, and J. R. Nix, Phys. Rev. C **17**, 2080 (1978).
[5]K. K. Gudima and V. D. Toneev, Yad. Fiz. **27**, 658 (1978) [Sov. J. Nucl. Phys. **27**, 351 (1978)]; **31**, 1455 (1980) [**31**, 755 (1980)].
[6]Y. Yariv and Z. Fraenkel, Phys. Rev. C **20**, 2227 (1979).

[7]J. Cugnon, T. Mizutani, and J. Vanderneulen, Nucl. Phys. **A352**, 505 (1981).
[8]V. E. Bunakov, Yad. Fiz. **25**, 505 (1977) [Sov. J. Nucl. Phys. **25**, 271 (1977)].
[9]T. N. Abutalybova, S. M. Kiselev, and Yu. E. Pokrovskii, Yad. Fiz. **38**, 1421 (1983) [Sov. J. Nucl. Phys. **38**, 865 (1983)].
[10]A. R. Bodmer, C. N. Panos, and A. D. Mackellar, Phys. Rev. C **22**, 1025 (1980).
[11]L. Wilets, E. M. Henley, M. Kraft, and A. D. Mackellar, Nucl. Phys. **A282**, 361 (1977); L. Wilets, Y. Yariv, and R. Chestnut, *ibid.* **A301**, 359 (1978).
[12]Y. Kitazoe, K. Yamamoto, and M. Sano, Lett. Nuovo Cimento **32**, 337 (1981).
[13]S. M. Kiselev, Yad. Fiz. **38**, 911 (1983) [Sov. J. Nucl. Phys. **38**, 547 (1983)]; S. M. Kiselev and Yu. E. Pokrovskii, *ibid.* **38**, 82 (1983) [*ibid.* **38**, 46 (1983)]; S. M. Kiselev, *ibid.* **39**, 32 (1984) [*ibid.* **39**, 18 (1984)]; Phys. Lett. **154B**, 247 (1985).
[14]J. J. Molitoris, J. B. Hoffer, H. Kruse, and H. Stocker, Phys. Rev. Lett. **53**, 899 (1984).
[15]G. S. Anagnostatos and C. N. Panos, Phys. Rev. C **26**, 260 (1982); **28**, 2546 (1983).
[16]G. S. Anagnostatos and C. N. Panos, Lett. Nuovo Cimento **41**, 409 (1984).
[17]G. Bertsch, J. Barysowicz, H. McManus, and W. G. Love, Nucl. Phys. **A284**, 399 (1977); G. R. Satchler and W. G. Love, Phys. Rep. **55**, 183 (1979).
[18]N. Isgur, Invited talk in the International Nuclear Physics Conference, Harrogate, U.K., 1986 (unpublished).
[19]G. S. Anagnostatos, Int. J. Theor. Phys. **24**, 579 (1985).
[20]C. N. Panos and G. S. Anagnostatos, J. Phys. G **8**, 1651 (1982).
[21]G. S. Anagnostatos, Lett. Nuovo Cimento **22**, 507 (1978); **28**, 573 (1980); **29**, 188 (1980); G. S. Anagnostatos, J. Yapitzakis, and A. Kyritsis, *ibid.* **32**, 332 (1981).
[22]J. P. Svenne, J. Phys. G **6**, 465 (1980).
[23]T. H. Koopman, Physica **1**, 104 (1933).
[24]H. S. M. Coxeter, *Regular Polytopes,* 3rd ed. (Macmillan, New York, 1973).
[25]G. S. Anagnostatos, C. N. Panos, I. E. Lagaris, V. A. Vutsadakis, and A. Kobos, Phys. Rev. C (in press).
[26]Y. Yariv and Z. Fraenkel, Phys. Rev. C **20**, 2227 (1979).
[27]S. Nagamiya, I. Tanihata, S. Schnetzer, L. Anderson, W. Bruckner, O. Chamberlain, G. Shapiro, and H. Steiner, J. Phys. Soc. Jpn. Suppl. **44**, 378 (1978); S. Nagamiya, L. Anderson, W. Bruckner, O. Chamberlain, M. C. Lemaire, S. Schnetzer, G. Shapiro, H. Steiner, and I. Tanihata, Phys. Lett. **81B**, 147 (1979).